WILEY polymers advanced technologies

Effects of polystyrene-*b*-poly(ethylene/propylene)-*b*-polystyrene compatibilizer on the recycled polypropylene and recycled high-impact polystyrene blends

Yufei Kong[1] | Yingchun Li[1] | Guosheng Hu[1] | Nuo Cao[2] | Youquan Ling[1] | Duo Pan[3,4] | Qian Shao[4] | Zhanhu Guo[3] (iD)

[1] School of Materials Science and Engineering, North University of China, Taiyuan 030051, China

[2] China National Electric Apparatus Research Institute Co, Ltd, Guangzhou 510000, China

[3] Department of Chemical and Biomolecular Engineering, University of Tennessee, Knoxville, TN 37996, USA

[4] College of Chemical and Environmental Engineering, Shandong University of Science and Technology, Qingdao 266590, China

Correspondence
Yingchun Li, School of Materials Science and Engineering, North University of China, Taiyuan 030051, China.
Email: liyingchun@126.com

Zhanhu Guo, Department of Chemical and Biomolecular Engineering, University of Tennessee, Knoxville, TN 37996, USA.
Email: zguo10@utk.edu

The recycled polypropylene/recycled high-impact polystyrene (R-PP/R-HIPS) blends were melt extruded by twin-screw extruder and produced by injection molding machine. The effects of polystyrene-*b*-poly(ethylene/propylene)-*b*-polystyrene copolymer (SEPS) used as compatibilizer on the mechanical properties, morphology, melt flow index, equilibrium torque, and glass transition temperature (T_g) of the blends were investigated. It was found that the notch impact strength and the elongation at break of the R-PP/R-HIPS blends with the addition of 10 wt% SEPS were 6.46 kJ/m^2 and 31.96%, which were significantly improved by 162.46% and 57.06%, respectively, than that of the uncompatibilized blends. Moreover, the addition of SEPS had a negligible effect on the tensile strength of the R-PP/R-HIPS blends. Additionally, the morphology of the blends demonstrated improved distribution and decreased size of the dispersed R-HIPS phase with increasing the SEPS content. The increase of the melt flow index and the equilibrium torque indicated that the viscosity of the blends increased when the SEPS was incorporated into the R-PP/R-HIPS blends. The dynamic mechanical properties test showed that when the content of SEPS was 10 wt%, the difference of T_g decreased from 91.72°C to 81.51°C. The results obtained by differential scanning calorimetry were similar to those measured by dynamic mechanical properties, indicating an improved compatibility of the blends with the addition of SEPS.

KEYWORDS

compatibilizer, recycled high-impact polystyrene, recycled polypropylene, SEPS

1 | INTRODUCTION

The rapid development of electronic and electrical equipment industry witnessed the increase of wasted electronic and electrical equipment (WEEE) plastics, whose annual output around the world reached 40 million tons according to the latest estimates.[1,2] To some extent, traditional treatment of waste plastics will not only result in the waste of resources but also lead to environmental pollution.[3,4] Fortunately, majority of WEEE plastics are still functional or slightly defective and thus can be reused for future life cycles.[5,6] Therefore, the recycling

of WEEE plastics is a mutual-beneficial pattern that can not only reduce the damage to the environment but also realize the recycling of resource.[7,8] Some literatures have reported that the major constituents of WEEE plastics include polypropylene (PP) and high-impact polystyrene (HIPS).[9-11] Recycling mixed plastics via the preparation of blends attracts increasing attention since the outstanding improvements such as impact strength and processability compared with the uncompatibilizing blends.[12,13]

Recycled polypropylene (R-PP) and recycled high-impact polystyrene (R-HIPS) are typically incompatible, because of different

molecular structures and condensed structures.[14] Therefore, the compatibility improvement of R-PP/R-HIPS blends is essential to achieve high mechanical properties to meet the requirements for actual applications. The traditional solution to increase the interfacial interaction among the phases is the incorporation of compatibilizers in reducing the interfacial tension.[15] The polymers (with similar chemical structure to PP and HIPS) are always used as compatibilizers to increase the interfacial interaction, thus improving the mechanical properties of the PP/HIPS blends.[16,17]

Polystyrene-b-poly(ethylene/butylene)-b-polystyrene copolymer (SEBS), a kind of triblock copolymer, is usually used as compatibilizers in increasing the interface interaction in the blends.[12,18,19] For example, Mural et al[18] examined the effects of SEBS compatibilizer content on the morphologies and mechanical properties of the postconsumer PP/HIPS blends. It was found that the addition of 5 wt% SEBS resulted in a decrease in the average dispersed domain size of postconsumer PP/HIPS (70/30) blends from 5.078 to 2.082 μm; ie, SEBS played a prominent role in compatibilization. Although the compatibility of postconsumer PP/HIPS blends was effectively improved, the notched impact strength and the tensile strength of the PP/HIPS compounds were only increased by 6.88% and 11.97%, respectively. Hong et al[20] found that the triblock copolymers SEBS and polystyrene-b-poly(ethylene/propylene)-b-polystyrene (SEPS) were used as the compatibilizers and tremendously improved the interfacial adhesion between polyphenylene oxide dispersed phase and isotactic PP continuous phase. Moreover, the compatibilization of SEPS was better than that of SEBS from the perspective of improving the mechanical property of the blends above. Similarly, SEPS was also used to improve the compatibility of R-PP/R-HIPS blends because of the miscibility of polystyrene in SEPS and HIPS matrix. Taking into account lower interfacial tension, the Poly(ethylene/propylene) block components in SEPS were expected to be miscible with PP phase.[21] Besides, SEPS can also improve the toughness of the R-PP/R-HIPS blends since SEPS belongs to a kind of thermoplastic elastomer. However, the use of SEPS as a compatibilizer for R-PP/R-HIPS blends has not been reported.

In this paper, the R-PP/R-HIPS blends were successfully prepared with SEPS acting as the compatibilizer. The aim of this paper is mainly to study the compatibilization of SEPS by comparing the mechanical properties, morphology, melt flow index (MFI), equilibrium torque, and the glass transition temperature (T_g) of the R-PP/R-HIPS blends. Through the comparison of notch impact strength and morphology, the toughening effect of SEPS was also studied.

2 | EXPERIMENT

2.1 | Materials

The R-PP and R-HIPS from end-of-life electrical equipment shell were provided by Xinhuanbao Resource Utilization Co, Ltd (Foshan, China). The pieces of R-PP and R-HIPS had a mean particle size of 5 mm. The SEPS (Kraton G-1730) was used as the compatibilizer and was purchased from Zhangmutou Huaxin Sales of Plastic Materials (Dongguan, China). The virgin PP (being used for TV sets shells) and virgin HIPS (being used for air conditioning shells) were supplied by Shanghai Kingfa Technology Development Co, Ltd (Shanghai, China), whose notched impact strengths were 2.92 and 6.20 kJ/m², respectively.

2.2 | Blend preparation

Polymers were previously dried for 8 hours at 70°C in a vacuum drying oven. The R-PP/R-HIPS/SEPS blends with the formulations being presented in Table 1 were prepared via a parallel twin-screw extruder (SHJ-36, Nanjing Chengmeng Chemical Machinery Co, Ltd, China) at 190°C to 210°C. The feed screw speed and the extruder screw speed were 25 and 85 rpm, respectively. After melt extrusion, the samples were obtained by granulation, then dried at 70°C for 8 hours, and injected into standard specimens by injection molding machine for mechanical property test. The injection temperature ranged from 185°C to 200°C.

2.3 | Mechanical testing

Izod impact testing was performed at room temperature using the K-TEST KXJU-22A impact tester according to IOS 180: 2000. All specimens were first notched with a notch of 45° angle and then tested with a 1-J hammer. The tensile testing was performed at 23°C according to ISO 527-1: 2012 using the SANS CMT6104 testing machine with the speed being 50 mm/min.

2.4 | Scanning electron microscope

The morphological analysis of the fracture surface of the blends was examined by a scanning electron microscope (SEM) (model DB235, FEI Co, Ltd, USA). The samples were cryogenically fractured in liquid nitrogen and were etched with tetrahydrofuran for 8 hours, and then the specimens were coated with gold layer before the morphology study at an acceleration voltage of 20 kV.

2.5 | Melt flow index and mix torque analysis

The melt flow rate tester (MTS ZRZ1452, Ningbo, China) was used to examine the MFI of the blends according to ISO 1133: 2005 at 230°C with a load of 2.16 kg. The mix torque analysis of the blends was evaluated on a torque rheometer (XSS-300, Kechuang Rubber and Plastic Machinery Co, Ltd, China) at 190°C, and the rotor speed was 50 rpm.

TABLE 1 The accurate formulations of R-PP/R-HIPS/SEPS blends

Sample	R-PP, wt%	R-HIPS, wt%	SEPS, wt%
1	70	30	0
2	70	30	1
3	70	30	5
4	70	30	10

Abbreviations: R-HIPS, recycled high-impact polystyrene; R-PP, recycled polypropylene; SEPS, polystyrene-b-poly(ethylene/propylene)-b-polystyrene copolymer.

2.6 | Dynamic mechanical analysis

The dynamic mechanical properties were tested by using the dual cantilever mode. The test temperature was in the range from −30°C to 150°C with a heating rate of 3°C/min and frequency of 10 Hz. The size of the sample used in the test was 80 mm × 10 mm × 4.2 mm.

2.7 | Differential scanning calorimetry analysis

The differential scanning calorimeter (METTLER DSC822e) was used to perform differential scanning calorimetry (DSC) analysis of the R-PP/R-HIPS/SEPS composites. The samples were ground into powder and then tested by vacuum drying for 12 hours. Indium was used to calibrate the temperature and enthalpy. High purity nitrogen (flow rate of 50 mL/min) was used to protect the sample (2-3 mg). The sample was heated to 200°C within 10 minutes to eliminate the thermal history and then cooled down to −10°C and heated to 200°C again. All the rates of temperature change were 10°C/min, and all the DSC curves were recorded.

3 | RESULT AND DISCUSSION

3.1 | Mechanical properties analysis

The notched impact strength of the R-PP/R-HIPS blends with the function of SEPS content is shown in Figure 1. It can be seen that the notched impact strength of the R-PP/R-HIPS blends is only 2.46 kJ/m^2, which is lower than that of the virgin PP and virgin HIPS with the notch impact strength being 2.92 and 6.20 kJ/m^2, respectively. This is due to the typical incompatibility of R-PP/R-HIPS blends.[22,23]

The notched impact strength was increased significantly when the SEPS compatibilizer was added into the blends in the preparation of R-PP/R-HIPS composites. Obviously, the notched impact strength exhibited a gradually increasing trend with increasing the SEPS content. The interfacial strength of the blends was improved under the compatibilizing effect of SEPS containing the chemical structures similar to that of PP and HIPS.[24] As a kind of thermoplastic elastomer,

SEPS can also improve the impact toughness of the R-PP/R-HIPS blends. Thus, the notched impact strength of blends was obtained. When the SEPS content was 10 wt%, the notched impact strength of the blends reached 6.46 kJ/m^2, which was 162.60% higher than that of the pure blends with the notch impact strength being 2.46 kJ/m^2.

The effects of SEPS content on the elongation at break and the tensile strength of blends are shown in Figures 2 and 3, respectively. The elongation at break of the blend increases with the increase of SEPS content, which is consistent with the change trends of notched impact strength. When the SEPS content is 10 wt%, the elongation at break of the R-PP/R-HIPS compounds is 31.96%, increased by 57.06%. The tensile strength is observed to increase first and then decrease with increasing the SEPS content.

The compatibility of the R-PP/R-HIPS blends was improved when the SEPS was used as compatibilizer, which resulted in the gradual increase of the elongation at break of the R-PP/R-HIPS compounds with increasing the SEPS content. Additionally, as a kind of elastomer, the addition of SEPS can cause the tensile strength of the R-PP/R-HIPS compounds decrease. Hence, the tensile strength of the blends

FIGURE 2 Elongation at break of the R-PP/R-HIPS/SEPS blends. R-HIPS, recycled high-impact polystyrene; R-PP, recycled polypropylene; SEPS, polystyrene-*b*-poly(ethylene/propylene)-*b*-polystyrene copolymer
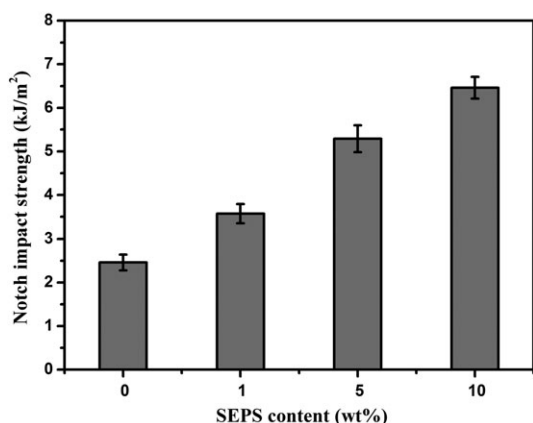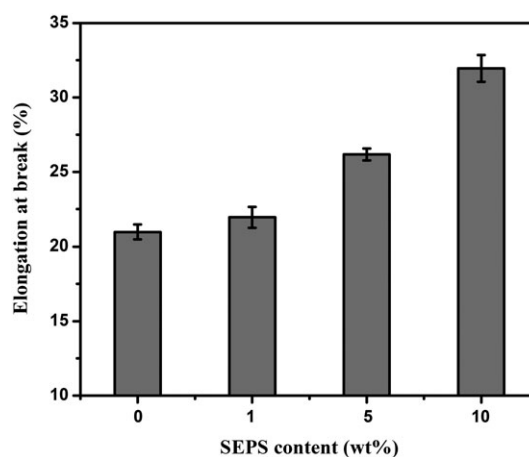
FIGURE 1 Notch impact strength of the R-PP/R-HIPS/SEPS blends. R-HIPS, recycled high-impact polystyrene; R-PP, recycled polypropylene; SEPS, polystyrene-*b*-poly(ethylene/propylene)-*b*-polystyrene copolymer
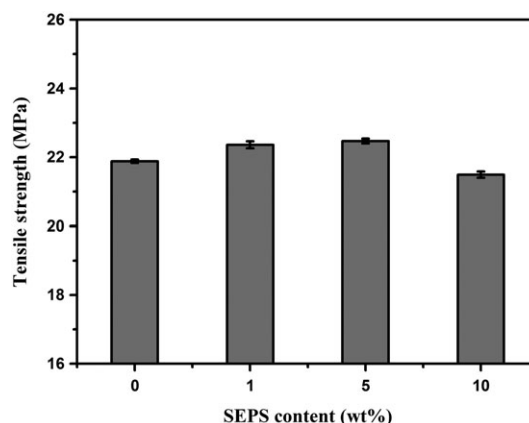
FIGURE 3 Tensile strength of the R-PP/R-HIPS/SEPS blends. R-HIPS, recycled high-impact polystyrene; R-PP, recycled polypropylene; SEPS, polystyrene-*b*-poly(ethylene/propylene)-*b*-polystyrene copolymer

began to decrease again, when the SEPS content exceeded 5 wt%. However, a slight decrease in tensile strength did not pose a new challenge to the reuse of the R-PP/R-HIPS composites.

3.2 | Morphology analysis

The SEM graphs of the brittle fracture surface of R-PP/R-HIPS compounds are shown in Figure 4. It is found that the morphology of the brittle fracture surface exhibits an obvious "sea-island" structure, where the gray part is the R-PP continuous phase and the black hole is the etched dispersed R-HIPS phase.[25,26] Without the addition of SEPS, the SEM graph of R-PP/R-HIPS blends shows an inhomogeneous distribution and irregular shape of the dispersed phase (Figure 4A). This is possibly attributed to the weak interfacial interaction among the phases in the blends. In general, high interfacial tension of the blends with poor compatibility will cause poor transformation of load from matrix to the dispersed phase, leading to a smooth morphology.[4,27]

Obviously, the compatibility of the blends was improved, which was illustrated by the morphology of the blends. A significant reduction of the R-HIPS domain size is found with SEPS as compatibilizer (Figure 4B-D). It is observed that the pore size is decreased considerably, which indicates the prominent compatibilization of the SEPS.

The possible reasons are that SEPS facilitates the dispersion of the R-HIPS dispersed phase and results in strong interfacial adhesion of the R-PP/R-HIPS blends.[28] This strong interfacial adhesive force may provide a better enhancement on the impact properties of the

blends. This observation confirms the effectiveness of SEPS as compatibilizer in intermediate R-PP/R-HIPS (70/30) blends. Through the addition of these compatibilizers, well-dispersed and small R-HIPS domains were obtained and exhibit excellent impact properties.

3.3 | Flow performance analysis

Melt flow index measurement has been used successfully to obtain significant information that is concerned about the viscosity of the R-PP/R-HIPS blends. Figure 5 shows the bar graph of MFI for all
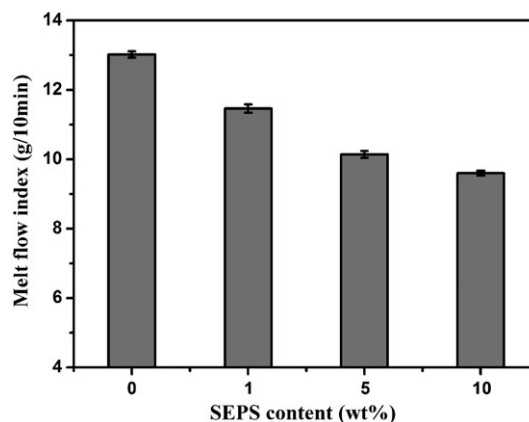

FIGURE 5 Melt flow index of the R-PP/R-HIPS/SEPS blends. R-HIPS, recycled high-impact polystyrene; R-PP, recycled polypropylene; SEPS, polystyrene-*b*-poly(ethylene/propylene)-*b*-polystyrene copolymer
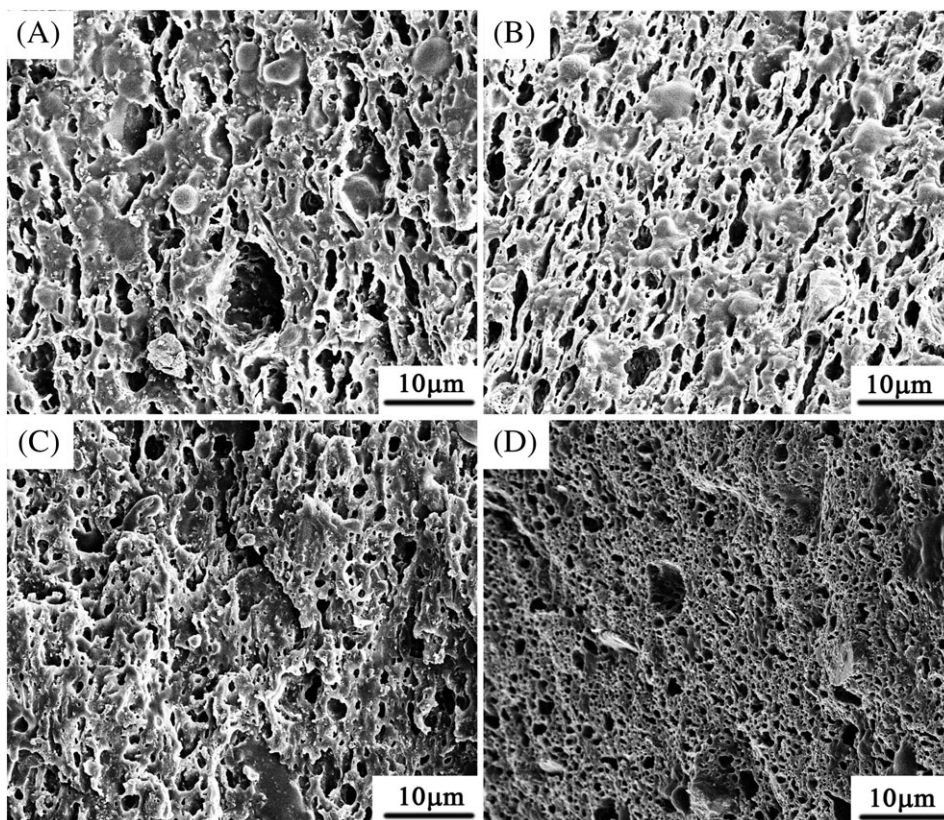

FIGURE 4 Scanning electron micrographs of the R-PP/R-HIPS/SEPS blends with a ratio of (A) 70/30/0, (B) 70/30/1, (C) 70/30/5, and (D) 70/30/10. R-HIPS, recycled high-impact polystyrene; R-PP, recycled polypropylene; SEPS, polystyrene-*b*-poly(ethylene/propylene)-*b*-polystyrene copolymer

samples. As can be seen, the MFI value of the blends reaches a maximum of 9.60 g/10 min when the content of SEPS is 10 wt%, which is much lower than the uncompatibilizing blends with the MFI value being 13.02 g/10 min. The MFI of the blends exhibits a decreasing trend with the increase of SEPS content, that is to say, the viscosity of the blends increases under the compatibilizing effect of SEPS. Figure 6 illustrates the effect of SEPS content on the equilibrium torque of R-PP/R-HIPS blends. Figure 6B is the enlarged diagram of the curve inside the dashed line of Figure 6A. The results show that the equilibrium torque of R-PP/R-HIPS blends without SEPS is 3.24 N·m, which is greater than that of the neat R-PP with the equilibrium torque being 2.71 N·m, but less than that of the neat R-HIPS whose equilibrium torque is 5.23 N·m. It is possibly due to the rigid benzene ring in R-HIPS molecules, which decreases the flow properties. With the increase of SEPS content, the equilibrium torque of the blends increases gradually. Decrease of MFI and increase of equilibrium torque of R-PP/R-HIPS blends shows that SEPS plays a vital role in compatibilizing R-PP/R-HIPS blends, which improves the interface strength between the dispersed phase and the continuous phase. The polystyrene block in SEPS is entangled with the polystyrene segments in the R-HIPS, and the polyethylene/PP block in SEPS is entangled with the PP chains in the R-PP, which leads to an increase

in viscosity of the blends. Figure 7 is the schematic representation of compatibilizer SEPS in the R-PP/R-HIPS blends. The more the SEPS content is, the higher the viscosity of the blends is observed, which is due to the positive correlation between the viscosity and the balance torque of the blends.[29,30] In addition, the changing trend of MFI and equilibrium torque is in accordance with the trend in the impact strength. When the SEPS compatibilizer is added into the blends, the interfacial interaction between the molecules of the blends described above is enhanced, resulting in the increased impact strength.

Tokita[31] has established the relationship between the particle size of the dispersed particles and the viscosity, shear rate, interfacial tension, volume fraction, the macroscopic crushing energy of the dispersed phase material, and the effective collision probability (Equation (1)):

$$R^* = \frac{\frac{12}{\pi}P\sigma\phi_d}{\eta\dot{\gamma} - \frac{4}{\pi}P\phi_d E_{dk}} \tag{1}$$

where R^* represents the particle size of the dispersed phase, P means the effective collision probability, σ is the interfacial tension, ϕ_d is the
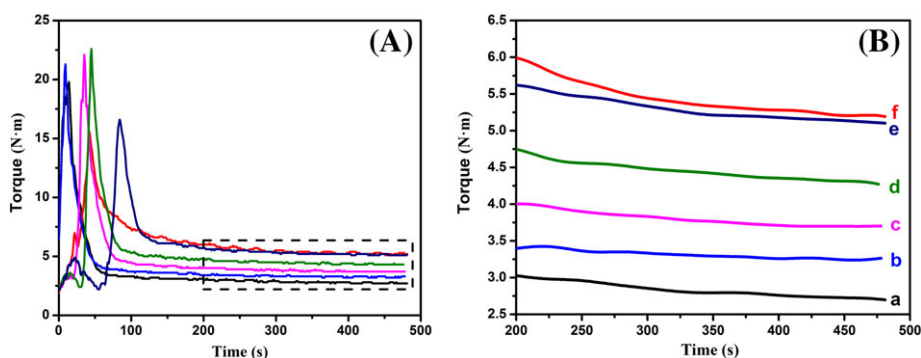

FIGURE 6 A and B, Mixing torque time of recycled polypropylene/recycled high-impact polystyrene/polystyrene-b-poly(ethylene/propylene)-b-polystyrene copolymer blends with a ratio of (a) 100/0/0, (b) 70/30/0, (c) 70/30/1, (d) 70/30/5, (e) 70/30/10, and (f) 0/100/0 [Colour figure can be viewed at wileyonlinelibrary.com]
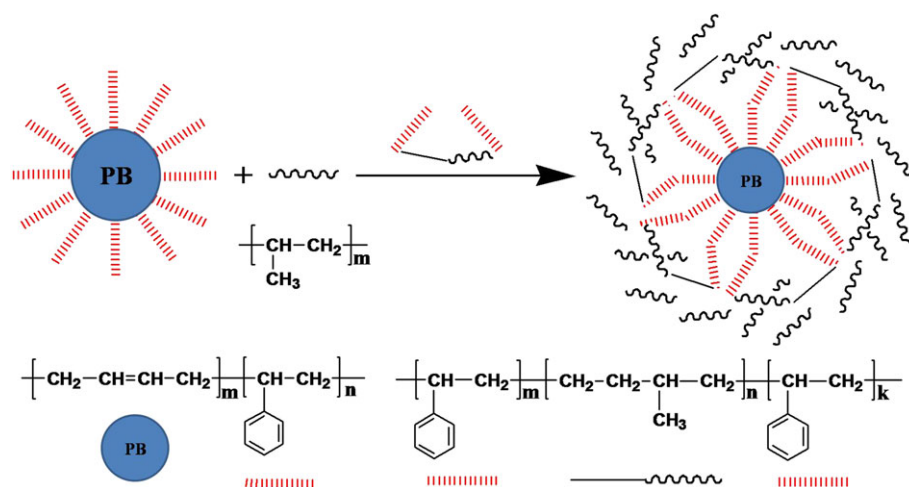

FIGURE 7 Schematic representation of compatibilizer polystyrene-b-poly(ethylene/propylene)-b-polystyrene copolymer in the recycled polypropylene/recycled high-impact polystyrene blends [Colour figure can be viewed at wileyonlinelibrary.com]

volume fraction of the dispersed phase, η represents the viscosity of the blends, and $\dot{\gamma}$ and E_{dk} are the shear rate and the macroscopic crushing energy of the dispersed phase material, respectively.

This formula is a classical formula for the blending process. The compatibilization of SEPS results in the decrease of effective collision probability of the dispersed phase and the decrease of the interfacial
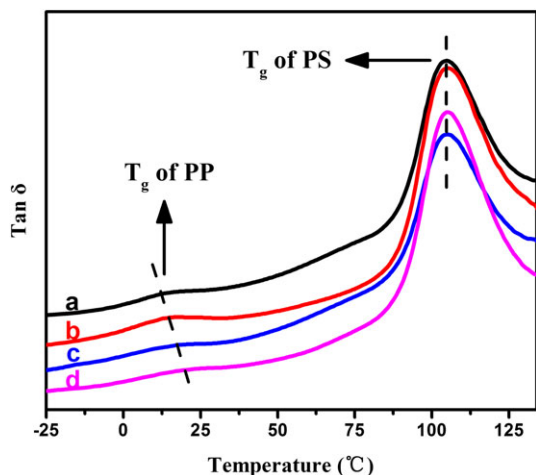
interaction among the phases, while the volume fraction of the dispersed phase and the shear rate remain unchanged; thus, the estimated particle size of the R-HIPS particles from Equation (1) is to be decreased. The results are in good agreement with the changes in the particle size observed by SEM in Figure 4, which matches the variation tendency of the impact strength. It indicates that SEPS has a prominent compatibilization effect on the notched impact strength and the elongation at break of R-PP/R-HIPS blends.

FIGURE 8 Glass transition temperatures of the R-PP/R-HIPS/SEPS blends from dynamic mechanical analysis measurements with a ratio of (a) 70/30/0, (b) 70/30/1, (c) 70/30/5, and (d) 70/30/10. R-HIPS, recycled high-impact polystyrene; R-PP, recycled polypropylene; SEPS, polystyrene-*b*-poly(ethylene/propylene)-*b*-polystyrene copolymer [Colour figure can be viewed at wileyonlinelibrary.com]

TABLE 2 Glass transition temperatures (T_g) of the R-PP/R-HIPS/SEPS blends from dynamic mechanical analysis measurements

Samples R-PP/R-HIPS/SEPS	T_g of R-PP, °C	T_g of R-HIPS, °C	Difference Value of T_g, °C
70/30/0	12.90	104.62	91.72
70/30/1	14.22	105.03	90.81
70/30/5	20.56	105.22	84.66
70/30/10	23.72	105.23	81.51

Abbreviations: R-HIPS, recycled high-impact polystyrene; R-PP, recycled polypropylene; SEPS, polystyrene-*b*-poly(ethylene/propylene)-*b*-polystyrene copolymer.
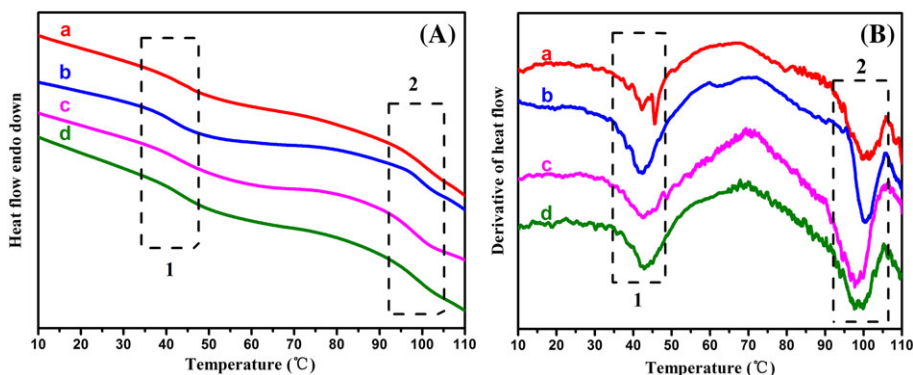
3.4 | Glass transition temperature

Figure 8 shows the temperature dependence of the tan δ curves of the R-PP/R-HIPS/SEPS blends with the data being presented in Table 2. As can be seen in Figure 8, 2 distinct transition peaks at 12.90°C and 104.62°C are found on the tan δ curves of the blends specimens, respectively, indicating that the R-PP and R-HIPS are incompatible. The peak of R-PP in the curve is not obvious, which is due to partial crystallization of the R-PP (it is a copolymerization PP that is derived from the waste electrical appliance). The difference of T_g between R-PP and R-HIPS is about 91.72°C. With the addition of SEPS, the T_g of R-PP increases and the temperature difference decreases. For example, when the content of SEPS is 10 wt%, the T_g of R-PP increases to 23.72°C, and the difference decreases to about 81.51°C. Additionally, the T_g of PS in R-HIPS increases slightly during the whole process.

Figure 9A shows the DSC curves of the second heats of R-PP/R-HIPS/SEPS blends. Figure 9B is obtained by the derivation of Figure 9 A with the data being presented in Table 3. In Figure 9B, it is shown that the 2 peaks in regions "1" and "2" correspond to the glass transition temperature of PP and polystyrene, respectively. In the blends without SEPS, the difference of T_g between R-PP and R-HIPS is about 58.91°C. When the SEPS content is increased, the difference of the blends decreases gradually and it reaches the minimum 55.32°C with the SEPS content being 10 wt%. Although the results of T_g obtained by DSC and dynamic mechanical analysis are different, the change tendency of the difference value is the same. The proximity of 2 glass transition temperatures above indicates that SEPS can significantly improve the compatibility of the R-PP/R-HIPS blends.[32,33]

FIGURE 9 A and B, Glass transition temperatures of the recycled polypropylene/recycled high-impact polystyrene/polystyrene-*b*-poly(ethylene/butylene)-*b*-polystyrene copolymer blends from differential scanning calorimetry measurements with a ratio of (a) 70/30/0, (b) 70/30/1, (c) 70/30/5, and (d) 70/30/10 [Colour figure can be viewed at wileyonlinelibrary.com]

TABLE 3 Glass transition temperatures (T_g) of the R-PP/R-HIPS/ SEPS blends from differential scanning calorimetry measurements

Samples R-PP/R-HIPS/SEPS	T_g of R-PP, °C	T_g of R-HIPS, °C	Difference Value of T_g, °C
70/30/0	42.11	101.02	58.91
70/30/1	42.22	100.26	58.04
70/30/5	42.62	98.78	56.16
70/30/10	42.84	98.16	55.32

Abbreviations: R-HIPS, recycled high-impact polystyrene; R-PP, recycled polypropylene; SEPS, polystyrene-*b*-poly(ethylene/propylene)-*b*-polystyrene copolymer.

4 | CONCLUSION

In this work, the R-PP/R-HIPS blends were prepared by melt extrusion. The R-PP/R-HIPS blends with SEPS compatibilizer exhibited the higher notch impact strength than that of the R-PP/R-HIPS blends. The SEM observations confirmed that a more homogeneous morphology of the compatibilizing R-PP/R-HIPS blends was achieved compared with the R-PP/R-HIPS blends without compatibilizers. The increase of the MFI and the decrease of the equilibrium torque indicate that the viscosity of the blends increased when the SEPS was used as compatibilizer, which was due to the improved compatibility of the blends. The dynamic mechanical analysis and DSC data proved that the addition of SEPS improved the compatibility of the R-PP/R-HIPS blends significantly, resulting in a close proximity of 2 glass transition temperatures belonging to the R-PP phase and R-HIPS phase, respectively. The R-PP/R-HIPS blends obtained excellent performance under the compatibilization of SEPS, which provided a new way for high value recycling of R-PP and R-HIPS to prepare multifunctional polymer nanocomposites[34-46] or carbon nanocomposites[47-52] upon pyrolysis.

ORCID

Zhanhu Guo http://orcid.org/0000-0003-0134-0210

REFERENCES

1. Ramesh V, Mohanty S, Biswal M, Nayak SK. Effect of reprocessing and accelerated weathering on impact-modified recycled blend. *J Mater Eng Perform*. 2015;24(12):5046-5053.

2. Mahanta D, Dayanidhi SA, Mohanty S, Nayak SK. Mechanical, thermal, and morphological properties of recycled polycarbonate/recycled poly(acrylonitrile-butadiene-styrene) blend nanocomposites. *Polym Compos*. 2012;33(12):2114-2124.

3. Kang H, Shao Q, Guo X, Galaska A, et al. Separation and recovery of copper foil and fabric from waste printed circuit boards by decomposing brominated epoxy resin using near critical water. *Eng Sci*. 2018, in press, doi: https://doi.org/10.30919/espub.es.180314. http://www.espublisher.com/doi/10.30919/espub.es.180312

4. Li YC, Wu XL, Song JF, et al. Reparation of recycled acrylonitrile-butadiene-styrene by pyromellitic dianhydride: reparation performance evaluation and property analysis. *Polymer*. 2017;124:41-47.

5. Menad N, Guignot S, Van Houwelingen J. New characterisation method of electrical and electronic equipment wastes (WEEE). *Waste Manag*. 2013;33(3):706-713.

6. Stenvall E, Tostar S, Boldizar A, Foreman MRS, Moller K. An analysis of the composition and metal contamination of plastics from waste electrical and electronic equipment (WEEE). *Waste Manag*. 2013;33(4):915-922.

7. Chen RQ, Jiang XL, You F, Yao C. Optimizing the morphology, mechanical and crystal properties of in-situ polypropylene/polystyrene blends by reactive extrusion. *Fiber Polym*. 2016;17(10):1550-1557.

8. Chung TH, Chang JY, Lee WC. Application of magnetic poly(styrene-glycidyl methacrylate) microspheres for immunomagnetic separation of bone marrow cells. *J Magn Magn Mater*. 2009;321(10):1635-1638.

9. Dimitrakakis E, Janz A, Bilitewski B, Gidarakos E. Small WEEE: determining recyclables and hazardous substances in plastics. *J Hazard Mater*. 2009;161(2-3):913-919.

10. Mishra S, Chatterjee A. Effect of nano-polystyrene (nPS) on thermal, rheological, and mechanical properties of polypropylene (PP). *Polym Advan Technol*. 2011;22(12):1547-1554.

11. Mishra S, Chatterjee A, Singh R. Novel synthesis of nano-calcium carbonate (CaCO3)/polystyrene (PS) core-shell nanoparticles by atomized microemulsion technique and its effect on properties of polypropylene (PP) composites. *Polym Advan Technol*. 2011;25:2571-2582.

12. Santana RMC, Manrich S. Morphology and mechanical properties of polypropylene/high-impact polystyrene blends from postconsumer plastic waste. *J Appl Polym Sci*. 2003;88(13):2861-2867.

13. Chen J, Hou YB, Zhang ML, et al. Combined effect of compatibilizer and carbon nanotubes on the morphology and electrical conductivity of PP/PS blend. *Polym Advan Technol*. 2014;25(6):624-630.

14. Huang HX, Xu HF. Preparation of microcellular polypropylene/polystyrene blend foams with tunable cell structure. *Polym Advan Technol*. 2011;22(6):822-829.

15. Wang D, Li Y, Xie XM, Guo BH. Compatibilization and morphology development of immiscible ternary polymer blends. *Polymer*. 2011;52(1):191-200.

16. Fortelný I, Michálková D, Hromádková J, Lednický F. Effect of a styrene-butadiene copolymer on the phase structure and impact strength of polyethylene/high-impact polystyrene blends. *J Appl Polym Sci*. 2001;81(3):570-580.

17. Aziz AA, Akil HM, Jamaludin SMS, Ramli NAM. The effect of multiple compatibilizers on the impact properties of polypropylene/polystyrene (PP/PS) blend. *Poly-Plast Technol Eng*. 2011;50(8):768-775.

18. Mural PK, Mohanty S, Nayak SK, Anbudayanidhi S. Polypropylene/high impact polystyrene blend nanocomposites obtained from E-waste: evaluation of mechanical, thermal and morphological properties. *Int J Plast Technol*. 2011;15(S1):46-60.

19. Macaúbas PH, Demarquette NR, Dealy JM. Nonlinear viscoelasticity of PP/PS/SEBS blends. *Rheol Acta*. 2005;44(3):295-312.

20. Hong XJ, Nie GT, Lin ZD, Rong JH. Structure and properties of PPO/PP blends compatibilized by triblock copolymer SEBS and SEPS. *Polym-Plast Technol*. 2012;51(10):971-976.

21. DeNicola Jr AJ, Guyer RA. Heat resistant composition of polyphenylene ether and/or polystyrene block copolymer (s) and styrenic grafted propylene polymer. Google Patents, 1994.

22. Li HM, Sui XW, Xie XM. High-strength and super-tough PA6/PS/PP/SEBS quaternary blends compatibilized by using a highly effective multi-phase compatibilizer: toward efficient recycling of waste plastics. *Polymer*. 2017;123:240-246.

23. Navas IO, Arjmand M, Sundararaj U. Effect of carbon nanotubes on morphology evolution of polypropylene/polystyrene blends: understanding molecular interactions and carbon nanotube migration mechanisms. *RSC Adv*. 2017;7(85):54222-54234.

24. Al-Saleh MH, Sundararaj U. Mechanical properties of carbon black-filled polypropylene/polystyrene blends containing styrene-butadiene-styrene copolymer. *Polym Eng Sci*. 2009;49(4):693-702.

25. Wu T, Yuan D, Qiu F, Chen RY, Zhang GZ, Qu JP. Polypropylene/polystyrene/clay blends prepared by an innovative eccentric rotor extruder based on continuous elongational flow: analysis of morphology, rheology property, and crystallization behavior. *Polym Test*. 2017;63:73-83.

26. Berahman R, Aghjeh MKR, Mazidi MM, Omrani S. Evolution of shell formation process in PP/PMMA/PS ternary blends: correlation between the melt rheology and phase morphology. *J Polym Res*. 2016;23:22701-22711.

27. Li YY, Wang Y, Li WQ, Sheng J. Compatibilization of styrene-butadiene-styrene block copolymer in polypropylene/polystyrene blends by analysis of phase morphology. *J Appl Polym Sci*. 2007;103(1):365-370.

28. Starý Z, Kruliš Z, Hromádková J, Šlouf M, Kotek J, Fortelný I. New multicomponent compatibilization system for polyolefin/polystyrene blends. *Int Polym Proc*. 2006;21(3):222-229.

29. Gao JG, Du YG, Dong CF. Rheological behavior and mechanical properties of blends of poly(vinyl chloride) with CP-POSS. *Int J Polym Mater*. 2010;59:15-24.

30. Liu Y, Li SC, Liu H. Melt rheological properties of LLDPE/PP blends compatibilized by cross-linked LLDPE/PP blends (LLDPE-PP). *Polym-Plast Technol*. 2013;52(8):841-846.

31. Tokita N. Analysis of morphology formation in elastomer blends. *Rubber Chem Technol*. 1977;50(2):292-300.

32. Thirtha V, Lehman R, Nosker T. Effect of additives on the composition dependent glass transition variation in PS/PP blends. *J Appl Polym Sci*. 2008;107(6):3987-3992.

33. Zhang Y, Huang Y, Mai K. Crystallization and dynamic mechanical properties of polypropylene/polystyrene blends modified with maleic anhydride and styrene. *J Appl Polym Sci*. 2005;96(6):2038-2045.

34. Ma YL, Lv L, Guo YR, et al. Porous lignin based poly(acrylic acid)/organo-montmorillonite nanocomposites: swelling behaviors and rapid removal of Pb (II) ions. *Polymer*. 2017;128:12-23.

35. Wang CF, Zhao M, Li J, et al. Silver nanoparticles/graphene oxide decorated carbon fiber synergistic reinforcement in epoxy-based composites. *Polymer*. 2017;131:263-271.

36. Zhao JB, Wu LL, Zhan CX, Shao Q, Guo Z, Zhang L. Influence of formamide and water on the properties of thermoplastic starch/poly(lactic acid) blends. *Polymer*. 2017;133:272-287.

37. Zhou P, Wang S, Tao CL, et al. PAA/alumina composites prepared with different molecular weight polymers and utilized as support for nickel-based catalyst. *Adv Polym Technol*. 2018. in press. doi:https://doi.org/10.1002/adv.21908

38. He YX, Yang S, Liu H, et al. Influence of formamide and water on the properties of thermoplastic starch/poly(lactic acid) blends. *J Colleoid Interf Sci*. 2018;517:40-51.

39. Yang WQ, Wang XL, Li JF, et al. Influence of formamide and water on the properties of thermoplastic starch/poly(lactic acid) blends. *Polym Eng Sci*. 2018. in press. doi:https://doi.org/10.1002/pen.24675

40. Cui XK, Zhu GY, Pan YF, et al. Polydimethylsiloxane-titania nanocomposite coating: fabrication and corrosion resistance. *Polymer*. 2018;138:203-210.

41. Gu H, Xu X, Zhang H, et al. Chitosan-coated-magnetite with covalently grafted polystyrene based carbon nanocomposites for hexavalent chromium adsorption. *Eng Sci*. 2018, in press, https://doi.org/10.30919/espub.es.180308. http://www.espublisher.com/doi/10.30919/espub.es.180308

42. Hu Z, Shao Q, Huang Y, et al. Light triggered interfacial damage self-healing of poly(p-phenylene benzobisoxazole) fiber composites. *Nanotechnology*. 2018;29(18):185602.

43. Guo Y, Xu G, Yang X, et al. Significantly enhanced and precisely modeled thermal conductivity in polyimide nanocomposites by chemically modified graphene via in-situ polymerization and electrospinning-hot press technology. *J Mater Chem C*. 2018;6(12):3004-3015.

44. Wang C, He Z, Xie X, et al. Controllable crosslinking anion exchange membranes with excellent mechanical and thermal properties. *Macromol Mater Eng*. 2018, in press, DOI: https://doi.org/10.1002/mame.201700462;303(3).

45. Wang X, Liu X, Yan H, et al. Non-covalently functionalized graphene strengthened poly(vinyl alcohol). *Mater Design*. 2018;139:372-379.

46. Lin J, Chen X, Chen C, et al. Durably antibacterial and bacterially anti-adhesive cotton fabrics coated by cationic fluorinated polymers. *ACS Appl Mater Interfaces*. 2018;10(7):6124-6136.

47. Zhang L, Yu W, Han C, et al. Large scaled synthesis of heterostructured electrospun TiO2/SnO2 nanofibers with an enhanced photocatalytic activity. *J Electrochem Soc*. 2017;164(9):H651-H656.

48. Zhang L, Qin MK, Yu W, et al. Heterostructured TiO$_2$/WO$_3$ nanocomposites for photocatalytic degradation of toluene under visible light. *J Electrochem Soc*. 2017;164(14):H1086-H1090.

49. Song B, Wang TT, Sun HG, et al. Two-step hydrothermally synthesized carbon nanodots/WO3 photocatalysts with enhanced photocatalytic performance. *Dalton Trans*. 2017;46(45):15769-15777.

50. Huang JN, Cao YH, Shao J, Peng XF, Guo ZH. Magnetic nanocarbon adsorbents with enhanced hexavalent chromium removal: morphology dependence of fibrillar vs particulate structures. *Ind Eng Chem Res*. 2017;56(38):10689-10701.

51. Gong KD, Hu Q, Yao L, et al. Ultrasonic pretreated sludge derived stable magnetic active carbon for Cr(VI) removal from wastewater. *ACS Sustain Chem Eng*. 2018. in press. doi:https://doi.org/10.1021/acssuschemeng.7b04421

52. Cheng CB, Fan RH, Wang ZY, et al. Tunable and weakly negative permittivity in carbon/silicon nitride composites with different carbonizing temperatures. *Carbon*. 2017;125:103-112.